Rich State Transitions in a Media Choreography Framework Using an Idealized Model of Cloud Dynamics

Brandon Mechtley
bmechtley@asu.edu
Synthesis
School of Arts, Media and Engineering
Arizona State University
Tempe, Arizona 85287

Julian Stein
jestein@asu.edu
Synthesis
School of Arts, Media and Engineering
Arizona State University
Tempe, Arizona 85287

Christopher Roberts
cmrober2@asu.edu
Center for Scholarship and Research Engagement
Regis University
Denver, Colorado 80221

Sha Xin Wei
xinwei.sha@asu.edu
Synthesis
School of Arts, Media and Engineering
Arizona State University
Tempe, Arizona 85287

ABSTRACT

This paper presents *An Experiential Model of the Atmosphere*, a responsive media environment including multi-surface video projection and ambisonic audio feedback in which participants can fluidly interact with an idealized model of atmospheric dynamics, using the presence and motion of their bodies to force convection, condense and evaporate moisture, and manipulate atmospheric pressure gradients. We use this model to explore steering of computational models of complex systems that can span gamuts of single to multi-body interaction, local to global spatial scales, short- to long-term time scales, and abstract representations to immersive, felt environments.

CCS CONCEPTS

• **Human-centered computing → Mixed / augmented reality**; **Gestural input**; *Collaborative interaction*; • **Applied computing** → *Performing arts*; *Media arts*;

KEYWORDS

media choreography, dense media, steerable simulation

1 INTRODUCTION

This paper describes the development of an architecture for an interactive media system that leverage inhabitants' kinesthetic intuition of physical matter to guide their interaction with new media systems. This platform integrates dense sensing and output modalities, controlled by an underlying model of a real-world complex system. In this paper, we focus on a particular application of this platform, an experiential model of atmospheric dynamics. This work is motivated by previous work in responsive and experiential media, dense media processing, and computational steering. To get a sense of the experiential environment, refer to videos in [15, 16].[1]

1.1 Responsive, dense media environments

Looking beyond the IoT epoch, we see that the complexity of our computationally mediated environments far exceed human cognitive capacities for explicit, tokenized communication and control. Rather than explicitly design discrete turn-taking interaction between human and machine, where at each step, the user or the machine chooses among a small number of discrete, pre-given choices, *responsive media* [19] are inspired by models of how humans work with continuous physical media such as air, water, clay, and sound. Responsive media are continuous fields of hybrids of physical or computational media (e.g. sound, light) that change continuously according to arbitrary continuous perturbation.[2] Such media behave gracefully in response to unanticipated human activity.

The density of sensors in many modalities is approaching what to human perception seems like a continuous distribution. The density of sensors in active textiles, thin films, and even distributions of photocells or physical sensors like radar will achieve densities approaching that of CCD. Audio sensing achieves sample rates of 44KHz and higher, and other modalities are beginning to increase orders of magnitude in time resolutions as well. On the output side, the actuation of physical matter together with time-based media will achieve time-space densities rivaling that of computationally modulated video and sound. This increase in sensing capability demands new paradigms for computation and interaction that enable the discovery and modulating of patterns of such *dense* environments.

ThematicWorkshops'17, October 23–27, 2017, Mountain View, CA, USA

ISBN 978-1-4503-5416-5/17/10…$15.00
DOI: https://doi.org/10.1145/3126686.3126771

[1] http://vimeo.com/synthesiscenter/videos/search:ema. See also https://vimeo.com/synthesiscenter/demo.

[2] This assumes that the media can be conceived of as topological space, on which a perturbation is said to be continuous if any inverse image of an open set is an open set [11].

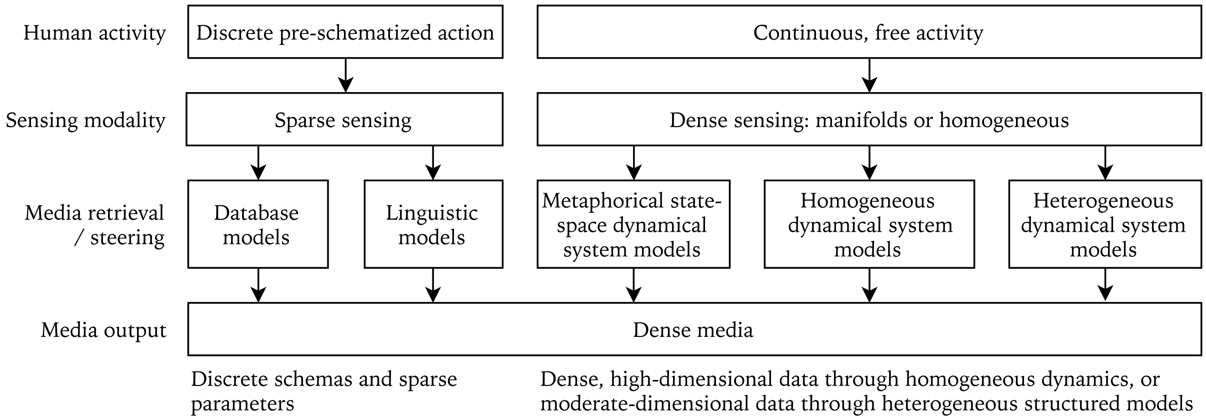

Figure 1: A comparison of sparse and dense sensing modalities for driving dense media, such as real-time audio or video projection. Sparse sensing uses discrete representations of pre-defined actions, such as individual gestures or words, as discrete tokens to represent human activity, whereas the dense media system described in this paper attempts to keep representations of activity and control of media states dense throughout the entire pipeline.

The goal behind developing architectures for dense media processing is to leverage people's pool of corporeal, pre-verbal intuition, acquired from infancy, about the behavior of continuous physical material to build rich engagement with dense environments. See [21, 23] for fuller justification on enactive and phenomenological grounds.

Computational platforms such as those described by [24] and [21] have been created for the purpose of integrating gestural interaction with densely complex models via dense multi-modal interfaces. In an era of rapid advances in active materials and new sensor capabilities, the main challenge to developing such systems is handling a density of data that approaches a continuous distribution. The general approach in these platforms has been to employ effectively continuous dynamical systems with which multiple users can concurrently interact gesturally or via whole-body interaction in multiple modalities.

Experiential media systems [17, 29] in general exploit human embodied capacity to engage creatively, exploratorily, and improvisatorily with dense environments. As Varela et al. [31] put it, "cognition is not the representation of a pregiven world by a pregiven mind but is rather the enactment of a world and a mind on the basis of a history of the variety of actions that a being in the world performs." This enactive approach to interactive media has been applied to multiple domains including live action in performative environments (dance, musical or theatrical performance, games) and movement/gesture tracking in everyday or health contexts. In this paper, we focus on the application of responsive, experiential media in the creation of an experiential atmospheric model.

1.2 Computational steering

The modeling of computational experiential media off participants' intuition of dense, continuous physical media is closely related to previous work in *computational steering*. In computational steering of simulations or operational environments, investigators change parameters of computational models on the fly and immediately receive feedback on the effect, in parallel with the execution of the simulation. Computational steering has been applied to the real-time control of complex scientific simulations, such as fluid dynamics [13], but has been extended to the realtime, human-in-the-loop modulation of any computationally-modulated environment where the results are immediately perceived [30, 32], thus minimizing the time between configuration and analysis of a simulation.

With advances in dense sensing modalities and experiential media, previous responsive media systems have expanded upon these primarily screen-based interactions in several aspects:

(1) Embodied enactive environments allow comparatively unconstrained, gestural, and full-body engagement with the computation.
(2) Applications range widely from basic experiential experiments (e.g. relation between memory and corporeal movement, or rhythmic entrainment of ensembles of people and time-based media processes) to artistic installations and performance (e.g. *Serra* [12] and *Timelenses* [27]).[3]
(3) Designing for whole body and ensemble engagement implies thick [18, 23], multimodal, analog and digital engagement with the environment as opposed to interacting along one or a few dimensions of sensorimotor perception.

2 STEERABLE SIMULATIONS IN A MEDIA CHOREOGRAPHY SYSTEM

A *media choreography system* [20, 22, 23] is generally a set of software frameworks (and hardware) that coordinate time-varying media—fields of light, video, sound, actuated materials or objects—in concert with the contingent activity of people in a given indoor or outdoor environment. A media choreography system comprises analog to digital devices (wearable, mobile, or fixed sensors; cameras; microphones; …), feature extraction, mapping or state logic, media synthesis instruments (sometimes distributed across a network of processors), and physical media devices (speakers, projectors, motorized objects, actuated materials, …) (see Figure 2b). A

[3] http://serracreation.weebly.com/, http://vimeo.com/synthesiscenter/palimpsest

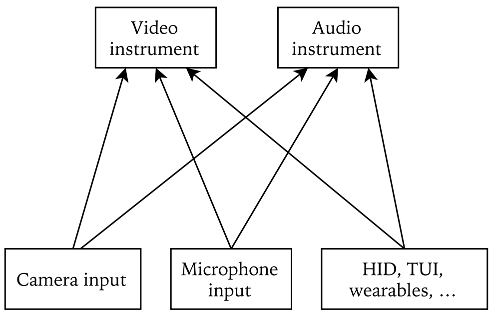

(a) An architecture for an audio-video experiential media system that uses manual, preprogrammed mappings between sensing modalities and audio and video instruments.

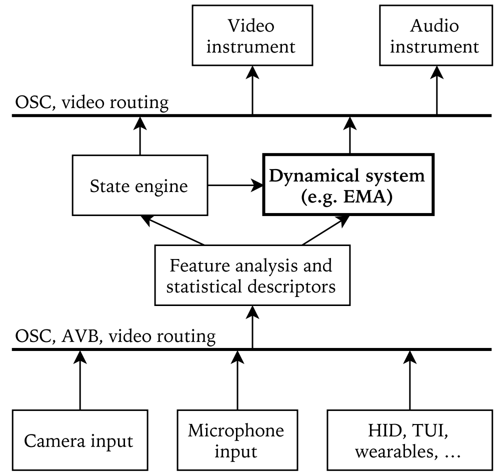

(b) An architecture for an audio-video media choreography system using high-level descriptors for potentially multimodal features to drive a state engine which guides transitions between states in audio and video instruments. In this paper, a dynamical system engine has been included which not only guides the instruments between several finite states but also provides dense, continuous phase transitions between media states.

Figure 2: Ozone media choreography system architecture.

key aspect of media choreography systems is that in order for the time-based media to feel like they are evolving in concert with arbitrary activity of the inhabitants, all computation of the "response" must take place under the threshold of latency that is imperceivable according to the sensory modality. This varies greatly according to sensory modality. For haptics and sound it can be on the order of 1 ms, placing tight bounds on real-time computation.

2.1 Designing media at the level of metaphor

The *continuous*, non-discrete, state-based media choreography system described in [24] presents a system for driving media states in several experiential media environments whereby multiple sensory modalities are used in conjunction to contribute to qualities of human activity at the level of metaphor. For example, concepts of "closeness" between moving bodies, "solo" activity, or "group" activity are made available to designers, independent of actual implementation in terms of specific sensors and computer vision or signal processing algorithms. In this way, the environments created with the system can evolve with new sensing technologies as new mappings to these qualities are produced by system architects. Additionally, [24] provides a level of metaphorical abstraction between design and implementation allowing for dramaturgical or aesthetic designers who are not familiar with the underlying programming to conceptually define compositions. A key element of this framework was also the inclusion of a dynamic *state engine*, a set of unique media states and state transitions defining a simplex in a high-dimensional space of media parameters, such as properties of a video or audio instrument, that allows media designers to map these metaphorical properties of human activity to distinct phase transitions in media. An architectural diagram of this type of system is shown in Figure 2a.

The media choreography system is also designed to leverage distributed computational resources, as CNMAT's *Open Sound Control* (OSC) protocol is encapsulated in UDP multicast datagrams to route continuous output from sensory mappings and remote control of media states. Additionally, video routing hardware is used to pass high-resolution, dense media between systems.

2.2 Integration of steerable simulations

In this work, we build upon the strategy of metaphorical mapping between activity and media states by interpolating a palpably rich, *continuously evolving* computational model of a complex system—in this case, an idealized model of atmospheric dynamics—that drives the media states, allowing for a wider range of phase transitions that can, in the case of a physical model, leverage the kinesthetic intuition of both designers and movers in the space. The architecture has thus been designed to allow for different complex system models to drive the phase transitions between media states. Figure 2b presents this new system architecture.

In addition to giving media designers a richer palette of possible system states, the inclusion of this additional layer to the system allows participants in the space to explore specific phenomena that can be recreated with the model. In the case of our atmospheric simulation, participants can use whole body interaction to directly force physical processes, such as convection, condensation, or evaporation, or steer the system toward emergent physical phenomena such as lee waves and cloud streets, microbursts, and fronts.

3 ATMOSPHERIC SIMULATION

Several methods have been developed for real-time cloud simulation, including procedural rendering techniques to produce forms that resemble specific types of clouds [3–6, 14, 33, 34] and physical modeling techniques that attempt to simulate atmospheric dynamics and microphysics [7, 9], akin to idealized models used in the rigorous study of atmospheric phenomena, e.g. [1]. The representative procedural techniques have been useful in gaming and virtual reality applications with a limited rendering budget than cannot devote instruction cycles to more complex models, and they are particularly useful for artists to be able to design clouds with predictable results. The latter models, however, despite being computationally expensive, explicitly allow for phase changes such as condensation and evaporation between condensed liquid and water vapor, and these realistic atmospheric dynamics lend themselves well toward highly expressive, responsive interaction that can better allow participants to interact with and gain an intuition for the complex dynamics of atmospheric *processes* in addition to forms.

We have based the two-dimensional simulation used in this piece on [9], which uses a computational fluid dynamics simulation to advect multiple densities—including potential temperature, water vapor, and condensed water—and model the phase changes in the mixing ratios of these phases of water and the subsequent effects on potential temperature. The following sections provide an overview of the different components of the mathematical model used, and we direct the reader to [9] and [26] for a more thorough overview of their numerical solution, as implementation details for the fluid dynamics used are widely available and the scope of this paper focuses more specifically on the mappings between human activity and simulation parameters. All processes have been implemented as fragment shaders executed on the graphics processor using Max/MSP/Jitter's *jit.gl.gen* abstraction, which uses a custom shader language that is later cross-compiled to GLSL code. Our implementation can be found on http://synthesiscenter.net/projects/ema.

3.1 Fluid dynamics

The underlying fluid dynamics follow the stable fluids method for incompressible flow from [26] and [8]. A semi-lagrangian scheme is used to advect the velocity of the fluid, $\mathbf{u}$, as well as three other densities, including the perturbation of potential temperature from an initial baseline, θ', and mixing ratios of water vapor, q_v, and condensed, liquid water, q_l.

In addition to fluid dynamics simulation parameters such as simulation speed, cell size, velocity and density dissipation, and vorticity, each of the environmental constants described below can be controlled at runtime, allowing not only changes to the simulated densities through movement, but also steerable control of environmental properties. Table 1 lists each of these environmental parameters as well as standard values used in our simulations.

The equations of motion are as follows:

$$\frac{\partial \mathbf{u}}{\partial t} = -(\mathbf{u} \cdot \nabla)\,\mathbf{u} - \frac{1}{\rho}\nabla p + \mathbf{B} + \mathbf{f_{ext}} \qquad (1)$$

$$\nabla \cdot \mathbf{u} = 0, \qquad (2)$$

Parameter	Description	Value
T_0	Base temperature	288.15 K
p_0	Base pressure	101.3 kPa
z_0	Altitude at origin	0 m
Γ	Temperature lapse rate	−6.5 K/km
c_{pd}	Specific heat of dry air at constant pressure	$1004\ \mathrm{J \cdot kg^{-1} \cdot K^{-1}}$
c_{vd}	Specific heat of dry air at constant volume	$717\ \mathrm{J \cdot kg^{-1} \cdot K^{-1}}$
c_{pv}	Specific heat of water vapor at constant pressure	$1850\ \mathrm{J \cdot kg^{-1} \cdot K^{-1}}$
c_{vv}	Specific heat of water vapor at constant volume	$1388.5\ \mathrm{J \cdot kg^{-1} \cdot K^{-1}}$
L_v	Latent heat of vaporization of water	$2.501 \times 10^6\ \mathrm{J \cdot kg^{-1}}$
$\mathbf{g}$	Gravity vector	$\langle 0, -9.8 \rangle\ \mathrm{m/s^2}$
$\mathbf{W}$	Wind vector	$\langle 0, 0 \rangle$ m/s
$\mathbf{O}$	Origin point in domain	$\langle 0, 0 \rangle$

Table 1: Runtime configurable environmental parameters with standard values from [28].

where ρ is the total fluid density, p is the computed fluid pressure, $\mathbf{B}$ is the buoyant acceleration due to gravity, and $\mathbf{f_{ext}}$ is total acceleration from all external forces, such as through user control. Equation 2 ensures the incompressibility of the fluid by enforcing zero divergence across the simulation domain.

The buoyancy force is handled differently from methods for simulating smoke, such as presented in [8] and [26], due to the presence of multiple phases of water which vary in density. Buoyancy is therefore modeled as in [1]:

$$\mathbf{B} = \mathbf{g}\left(\frac{\theta'}{\theta_0} + \left(\frac{1}{\varepsilon} - 1\right) q_v - q_l\right), \qquad \varepsilon = \frac{\Re_d}{\Re_v} \qquad (3)$$

where $\mathbf{g}$ is the gravity vector with magnitude equal to the acceleration due to gravity, θ_0 is the baseline potential temperature value, $\Re_d = c_{pd} - c_{vd}$ is the gas constant for dry air, and $\Re_v = c_{pv} - c_{vv}$ is the gas constant for water vapor. Water vapor will tend to rise when surronded by dry air, whereas parcels with high ratios of condensed water will be forced in the direction of gravity.

3.2 Moisture content

In addition to the equations of motion that govern the spatial dynamics of the fluid, [9] uses a bulk water continuity equation to conserve the total mass of water by ensuring that the rates of evaporation and condensation are balanced:

$$\frac{\partial q_v}{\partial t} + (\mathbf{u} \cdot \nabla)\, q_v = -\left(\frac{\partial q_l}{\partial t} + (\mathbf{u} \cdot \nabla)\, q_l\right) = -C, \qquad (4)$$

where C is the rate of condensation.

To compute the condensation rate for each frame, the Clasius-Clapeyron equation is used to compute the saturation vapor pressure [28]:

$$e_s \approx 0.611 \cdot \exp\left(\frac{L_v}{\Re_v}\left(\frac{1}{273.15} - \frac{1}{T}\right)\right), \quad T = \theta\left(\frac{p}{p_0}\right)^{\Re_v / c_{pv}}, \quad (5)$$

where environmental pressure, p, is computed from initial temperature that decreases with altitude according to an environmental lapse rate, as in [9]. L_v is the latent heat released from vaporization of water and c_{pv} is the specific heat capacity of water vapor at constant pressure at 15 °C. The saturation mixing ratio is then

$$r_s = \frac{\varepsilon \cdot e_s}{p - e_s}, \quad (6)$$

from which the condensation rate can be computed as in [9]:

$$C = -\min(r_s - q_v, q_l). \quad (7)$$

3.3 Thermodynamics

As water vapor within a parcel of air condenses, latent heat is released which warms the parcel. Following [9] and [10], this latent heat is modeled as follows:

$$\frac{\partial\theta}{\partial t} + (\mathbf{u} \cdot \nabla)\theta = \frac{L_v}{c_{pd}}\left(\frac{p_0}{p}\right)^{\Re_d / c_{pd}} C, \quad (8)$$

where L_v is the latent heat released from vaporization of water, p_0 is the standard atmospheric pressure at sea level and c_{pd} is the specific heat capacity of dry air at constant pressure.

3.4 Boundary conditions

For our simulation, optional binary masks for velocity, moisture content, and potential temperature can be used to enforce containment within the simulation domain using no-slip boundary conditions, without which periodic boundary conditions are assumed, allowing quantities to be advected from one side of the simulation to the other in both dimensions, as on the surface of a torus.

In our floor-projected simulations, typically quantities are not conserved within the domain and are allowed to drain at the edges. In our tests with vertical projections, a no-slip boundary is used at the bottom edge ($z = 0$) and periodic boundaries can be used for the sides along with a nonzero horizontal wind vector to create a continuous flow of clouds that can be shaped by movers in the space.

3.5 GPU implementation in Max/MSP/Jitter

All of the numerical solutions to the above equations are simulated on graphics hardware using the *jit.gl.gen* object within the visual data-flow programming environment Max/MSP/Jitter, which is then cross-compiled to GLSL.

4 MULTIMODAL FEEDBACK

An Experiential Model of the Atmosphere (EMA) is implemented in a 25x25-foot black box research space for the construction of responsive media environments. In addition to a networked media choreography system including multiple media processing computers, flexible audio and video routing through audio-video-bridge (AVB) networking, and a Blackmagic Videohub, the space has reconfigurable floor, wall, and scrim projections, an 8-channel speaker array, high-definition infrared optical tracking with side- and ceiling-mounted Point Grey cameras, a DMX-controllable lighting grid, and a host of wearable sensing technologies for developing embodied interactions.

For *EMA*, we have used the optical sensing, multi-surface projection, and spatialized audio capabilities to provide embodied steering of the atmospheric simulation with multimodal feedback. Our initial experiments with *EMA* have involved running two parallel simulations, one of which uses a ceiling-mounted camera and floor projection, simulated at a constant height without gravitational force, and another simulation which uses a side-mounted camera and scrim projection to explore the dynamics at varying altitude.

4.1 Visual feedback: representational and immersive media

To explore the expressive capabilities of the media steered by the atmospheric model, we have built multiple video instruments that use the various fields of the model in multiple ways.

4.1.1 Abstract data visualization. First, to allow participants to explore the various facets of the model in the manner of traditional data visualization, we have created an interface on a wireless tablet computer that communicates with the simulation via OSC to switch between visualized quantities. Each field can then be viewed independently, such as the magnitude and direction of the velocity field, with velocity mapped onto a color wheel with varying intensity, the degree of quantities such as vorticity and divergence of the velocity field, and temperature, visualized through a heat map.

4.1.2 Representational media. We have also developed a visualization mode wherein mixing ratios of condensed water and water vapor are visualized concurrently to artificially resemble clouds. Simulating the scattering of light through water particles has been explored in other works simulating clouds, e.g. [9], but we have opted directly visualize the two separate quantities, allowing participants to understand the spatial distribution of the data, as shown in Figure 2a.

4.1.3 Immersive, non-representational media. We have also explored using the fields of the model not to visualize data, in the traditional sense, but to drive an immersive video instrument that mixes layers of continuously evolving video according to the relative mixing ratios and turbulence of the air. A video of a thunderstorm, associated with high convergence of the velocity field and high levels of condensed water, is continuously mixed with videos of barren desert landscape, associated with low water vapor and condensation, and stratus clouds, mapped to high water vapor and condensation. The video speed can then be modulated according to the magnitude of the velocity field.

4.2 Auditory feedback: sonification of fluid velocity and condensation

An audio instrument for the model has been developed such that multiple fields (and changes thereof) can effectively be heard at once, allowing inhabitants of the space to not only grasp the current

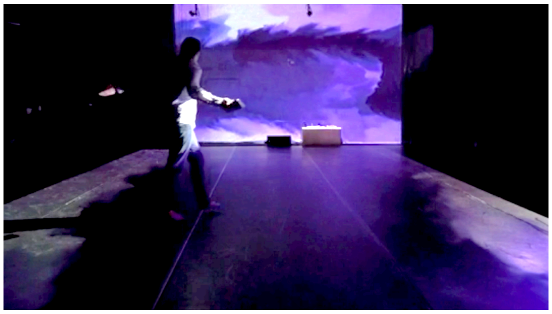

(a) A participant explores condensation and evaporation through cooling the simulated atmosphere as a function of their movement.

(b) Two participants act as an obstacles to laminar fluid flow, viewing the magnitude of the velocity field.

Figure 3: Immersive and representational visual feedback.

state of the model but also the trajectory of phase changes between condensed water and vapor. Ambisonic feedback has been used such that the location of these changes can also be determined.

Sonification of the model uses a rich audio instrument from [12], wherein multiple voices using a concatenative synthesis sampling engine are fed through a bank of resonant bandpass filters with adjustable center frequency and bandwidth and then spatialized with an 8-channel speaker array using IRCAM's *Spat* [2] real-time spatialization package.

For the atmospheric model, each field (such as water mixing ratios, velocity, or temperature) is down-sampled to a small number of grid cells, each of which drives the parameters for a single voice. We have found a mapping that sonifies the fluid velocity, vorticity, and condensation rate particularly effective, as listeners are able to distinguish between high and low wind speed, turbulent and laminar flow, and sudden changes in water phase.

For the velocity field, seeding sounds of wind, with decreasing bandwidth and greater volume at higher velocities, can produce the effect of high wind speeds, while decreasing the time between concatenated samples as a result of increased vorticity can produce the sensation of a more turbulent flow. For a positive condensation rate, we have explored using bright, crystalline ambiences, while for a negative condensation rate, we have used sounds with broadband spectra (close to white noise) that quickly move from low to high fliter bandwidth and decrease in volume to effect diffusing matter.

5 CONCEPTUAL MAPPINGS OF ACTIVITY FOR STEERING

The use of a physical model of atmospheric dynamics allows for a rich palette of interactive scenarios, as fluid flow, pressure, phase changes, external forces, gravity, and variations in altitude can all be used in conjunction with human movement and gesture to "paint" atmospheric phenomena and responsively explore the state space of the simulation. We have developed several mappings between human movement and simulation parameters to create a number of interactive scenarios that allow single participants and collaborative interactions between multiple participants to steer the simulation in novel ways.

5.1 Optical sensing and motion analysis

Embodied interaction with the system is enabled through analysis of camera input available in the Ozone system including adaptive background subtraction and optical flow estimation to obtain a velocity field of moving bodies, which can be used both to force fluid flow in the model and model bodies as dynamic obstacles using free-slip boundary conditions.

5.1.1 Optical flow and dynamic boundaries. To compute optical flow, the Horn-Schunk optical flow estimation is used as in the *cv.jit.HSflow* implementation. Two mappings to simulation parameters are available from this quantity, including external forcing of air velocity and use in conjunction with modeling of dynamic obstacles from the outline of bodies and objects in the space such that the optical flow of these outlines can be used as a proxy for the velocity along the perimiter of the non-rigid-body obstacles. These outlines are obtained through creating a binary mask from thresholding nonstationary or recently introduced features in camera input. An adaptive background subtraction takes the frame difference between the current frame of camera input with a low-pass filtered version to pick up only recent objects, allowing stationary features in the camera input to blend into the background, after which the input is convolved with a two-pass gaussian kernel of variable width and finally thresholded to form a binary image of recent features. Optical flow can then be computed on this binary mask, rather than the raw camera input, to obtain the velocity at the edges of the boundary.

5.2 Re-creating atmospheric phenomena with the body

5.2.1 Convection. Participants can use full-body movements to provide an external force on the fluid dynamics of the model. Similar to the techniques in [25] and [21], optical flow can be estimated from each camera feed using the Horn-Schunk method, computed on the graphics processor. This optical flow field can then be scaled and added to the total external forces, $\mathbf{f}_{\mathbf{ext}}$ in Equation 1.

We have explored using this mapping to allow participants to "force" the convective process of the atmosphere, in conjunction with visualization of the temperature field, to demonstrate the mixing of potential temperature in the atmosphere and the resulting condensation effect of forcing lift on a moist parcel of air. For example, one can use broad circular upward motions of the arms to create a periodic sheet of clouds in the presence of a constant force (or "wind") parallel to the floor.

5.2.2 Condensation and evaporation. In addition to exploring condensation effects from externally forcing lift, we have directly mapped the magnitude of optical flow to a reduction in the potential temperature field, reducing the modeled saturation mixing ratio and allowing water to condense. In this way, one can dynamically "paint" clouds in the simulation, resulting both in visual and auditory changes to the environment as the condensation rate results in sonic feedback.

5.2.3 Flow surrounding solid bodies. We have also mapped the boundaries of bodies moving in the space to solid obstructions to the fluid dynamics simulation. In these cases, the obstacles are treated as dynamic, using optical flow to account for their motion in order to model a free-slip boundary condition on a moving obstacle as discussed in [8]. In these experiments, participants are able to observe the resulting vortex sheets produced around their bodies, and many people can work together to observe the effects of increasing and decreasing the air velocity as it flows through narrower and wider channels, resulting in greater or lesser air pressure.

5.3 Spatiotemporal scaling by interpersonal distance

We have also experimented with varying the dynamics of the system according to single-participant and ensemble action through using the concept of "closeness" between movers in the space to control the spatial scale of the model in km/pixel. By using the blob-detection capabilities of *cv.jit* on top of the adaptive background subtraction method mentioned earlier, we obtain the centroids of each mover in the space and compute the smallest bounding box containing each centroid. We can then map the area of this bounding rectangle, scaled by a controlled parameter, to allow users to explore the dynamics of smaller spatial scales as they move together and larger spatial scales as they move apart. We have also experimented with mapping this quantity to the timestep of the model, allowing users to slow down the model in order to reflect on the state of the simulation and discuss the effects of their actions when they are close together.

6 CONCLUSIONS

In this paper, we have described a novel architecture for media choreography that allows for continuous phase transitions in multiple modalities of feedback in an experiential media system through the development of a simulation of atmospheric dynamics that can be steered through the activity of the space's inhabitants. Driving media states with this continuous dynamical system allows for a highly varied space of possible media states, which can intuitively be reached by participants through the similarity of the model's dynamics to physical matter. In addition to being able to steer the model directly through interactions such as forcing flow velocity with full-body movement, multiple atmospheric processes and forms can be attained, and higher-level concepts such as the closeness of participants in the space can be used to steer the system. We have explored a number of experiments both with creating mappings for steering the model and for providing visual and auditory feedback that use the model's various properties, ranging from traditional, abstract data representations to immersive, non-representational media instruments.

While a number of possibilities still remain for the use of *EMA*, it is only one of many possible systems that can be realized using a media choreography architecture that leverages steerable complex system dynamics, and moving beyond physical models, other models, including models of ecological and social systems may also prove fruitful, both for the purpose of interactive steering for the purpose of model investigation and for the purpose of driving responsive media environments.

ACKNOWLEDGMENTS

The authors would like to thank Drs. Melissa Bukovsky and Linda Mearns from the Regional Integrated Sciences Collective group at the National Center for Atmospheric Research (NCAR) for advising on atmospheric phenomena and providing much-needed feedback on the interactive media system. Much of the initial design of the simulation described in this paper was developed at NCAR through the support of the CISL Visitors Program (CVP). We thank Connor Rawls, Megan Patzem, Keyaanna Pausch, Garrett Johnson, and other students at Synthesis for their participation. We thank also the Provost and the Office of Knowledge Enterprise Development at ASU and the Carnegie Humanities Investment Fund for supporting Synthesis.

REFERENCES

[1] George H Bryan and J Michael Fritsch. 2002. A benchmark simulation for moist nonhydrostatic numerical models. *Monthly Weather Review* 130, 12 (2002), 2917–2928.

[2] T. Carpentier, M. Noisternig, and O. Warusfel. 2015. Twenty years of IRCAM Spat: looking back, looking forward. In *Proceedings of the 41st International Computer Music Conference (ICMC)*. Denton, TX.

[3] Yoshinori Dobashi, Tomoyuki Nishita, and Tsuyoshi Okita. 1998. Animation of clouds using cellular automaton. In *Proceedings of Computer Graphics and Imaging '98*. 251–256.

[4] Pantelis Elinas and Wolfgang Stürzlinger. 2000. Real-time rendering of 3d clouds. *Journal of Graphics Tools* 5, 4 (2000), 33–45.

[5] Robert Fizimayer. *A Real-Time Cloud Animation and Illumination Method.* Ph.D. Thesis. Technischen Universität Wien.

[6] Geoffrey Y. Gardner. 1985. Visual simulation of clouds. *ACM SIGGRAPH Computer Graphics* 19, 3 (1985), 297–304. DOI: https://doi.org/10.1145/325165.325248

[7] Robert Geist, Jay Steele, and James Westall. 2007. Convective Clouds. In *Proceedings of the Third Eurographics Workshop on Natural Phenomena*, D. Ebert and S. Mérillou (Eds.). Eurographics Association, 23–30.

[8] Mark J. Harris. 2004. Fast Fluid Dynamics Simulation on the GPU. In *GPU Gems: Programming Techniques, Tips and Tricks for Real-Time Graphics* (1 ed.), Randima Fernando (Ed.). Addison-Wesley Professional.

[9] Mark J. Harris, William V. Baxter III, Thorsten Scheuermann, and Anselmo Lastra. 2003. Simulation of cloud dynamics on graphics hardware. *Graphics Hardware* (2003), 92–102. DOI: https://doi.org/10.1145/1198555.1198793

[10] Robert A. Houze. 1993. *Cloud Dynamics.* Academic Press, San Diego, CA.

[11] Klaus Jänich. 1980, 1984. *Topology.* Springer-Verlag, Berlin. an exquisitely motivated, informal intuitive introduction to a wide swath of topology.

[12] Oana Suteu Khintirian. 2016. Serra Vegetal Life. (2016). http://serracreation.weebly.com/

[13] Oliver Kreylos. 1999. Computational Steering of CFD Simulations. (1999). http://idav.ucdavis.edu/~okreylos/ResDev/CFDSteering/index.html

[14] Horng-Shyang Liao, Tan-Chi Ho, Jung-Hong Chuang, and Cheng-Chung Lin. 2005. Fast rendering of dynamic clouds. *Computers & Graphics* 29, 1 (2005), 29–40. DOI: https://doi.org/10.1016/j.cag.2004.11.005

[15] Brandon Mechtley. 2017. *An Experiential Model of the Atmosphere.* Technical Report. Synthesis, ASU. https://vimeo.com/synthesiscenter/videos/search:ema

[16] Brandon Mechtley. 2017. videos of experiential complex systems. (2017). https://vimeo.com/synthesiscenter/videos/search:ema

[17] Thanassis Rikakis, Jiping He, Hari Sundaram, Gang Qian, and Andreas Spanias. 2005. An interdisciplinary arts and engineering initiative for experiential multimedia. In *ASEE Annual Conference and Exposition*. ASEE, 8715–8724.

[18] Sha Xin Wei. 2002. Future Physical Wear Me!!! Sha Xin Wei (US) - T-Garden project development. (June 2002). http://www.futurephysical.org/pages/content/wearable/wearme/info_processdemo_061202_dl_shaxinwei.htm

[19] Sha Xin Wei. 2002. Resistance Is Fertile: Gesture and Agency in the Field of Responsive Media. *Configurations* 10, 3 (2002), 439–472.

[20] Sha Xin Wei. 2006. *Ethico-Aesthetics in T* Performative Spaces*. Bezjak Tisk Maribor, Brussels, 22–39.

[21] Sha Xin Wei. 2010. Calligraphic Video: Using the Body's Intuition of Matter. *International Journal of Creative Interfaces and Computer Graphics* 1, 1 (2010), 67–83. DOI: https://doi.org/10.4018/jcicg.2010010106

[22] Sha Xin Wei. 2011. *Poetic and Speculative Architectures in Public Space*. AI and Society, Vol. 26.2. Springer-Verlag, London.

[23] Sha Xin Wei. 2013. *Poiesis, Enchantment, and Topological Matter*. MIT Press, Cambridge, MA.

[24] Sha Xin Wei, Michael Fortin, Navid Navab, and Tim Sutton. 2010. Ozone : Continuous State-based Media Choreography System for Live Performance. In *Proceedings of the ACM International Conference on Multimedia (SIGMM)*. 1383–1392. DOI: https://doi.org/10.1145/1873951.1874221

[25] Sha Xin Wei, Michael Fortin, and Jean-Sébastien Rousseau. 2009. Calligraphic video: a phenomenological approach to dense visual interaction. *Proceedings of the International Conference on Multimedia (SIGMM)* (2009), 1091–1100. DOI: https://doi.org/10.1145/1631272.1631518

[26] Jos Stam. 1999. Stable Fluids. In *Proceedings of the 26th Annual Conference on Computer Graphics and Interactive Techniques*. 121–128. DOI: https://doi.org/10.1145/311535.311548

[27] Julian Stein, Oana Suteu Khintirian, Todd Ingalls, and Sha Xin Wei. 2016. Time Lenses Apparatus. (2016). http://rhythmanalysis.weebly.com/time-lenses-apparatus.html

[28] Roland Stull. 2015. *Meteorology for Scientists and Engineers* (3rd ed.). University of British Columbia, Vancouver, BC.

[29] Hari Sundaram. 2013. Experiential Media Systems. *ACM Trans. Multimedia Comput. Commun. Appl.* 2, 3 (2013).

[30] Robert van Liere, Jurriaan D. Mulder, and Jarke J. van Wijk. 1996. *Computational steering*. Springer Berlin Heidelberg, Berlin, Heidelberg, 696–702. DOI: https://doi.org/10.1007/3-540-61142-8_616

[31] Francisco J. Varela, Evan Thompson, and Eleanor Rosch. 1991. *The Embodied Mind: Cognitive Science and Human Experience*. MIT Press, Cambridge, Mass.

[32] J. S. Vetter. 1997. Computational Steering Annotated Bibliography. *SIGPLAN Not.* 32, 6 (June 1997), 40–44. DOI: https://doi.org/10.1145/261353.261359

[33] Niniane Wang. 2004. Realistic and fast cloud rendering. *Journal of Graphics Tools* 9, 3 (2004), 21–40. DOI: https://doi.org/10.1080/10867651.2004.10504895

[34] Jamie Wither, Antoine Bouthors, and Marie-Paule Cani. 2008. Rapid sketch modeling of clouds. In *Eurographics Workshop on Sketch-Based Interfaces and Modeling (SBIM)*. Eurographics Association, 113–118.